

Short communication

## Lead-acid cells with lightweight, corrosion-protected, flexible-graphite grids

B. Hariprakash<sup>a,\*</sup>, S.A. Gaffoor<sup>b</sup>

<sup>a</sup> *Solid State and Structural Chemistry Unit, Indian Institute of Science, Sir C.V. Raman Avenue, Bangalore-560 012, India*

<sup>b</sup> *NED Energy Ltd., 6-3-1109/1 Navbharat Chambers, Raj Bhavan Road, Hyderabad-500 082, India*

Received 20 March 2007; received in revised form 11 April 2007; accepted 20 April 2007

Available online 27 April 2007

### Abstract

Lightweight grids for lead-acid battery plates are prepared from flexible graphite sheets of mass density  $1.1 \text{ g cm}^{-3}$ . The grids are coated with a lead layer followed by a corrosion-resistant polyaniline layer by electrodeposition. The grids are about 70% lighter than conventional lead-acid battery grids. The suitability of these grids are evaluated by cyclic voltammetric experiments. Lead-acid cells are assembled with positive and negative plates made from these lightweight grids. The specific energy of the lead-acid cells is found to be *ca.*  $40 \text{ Wh kg}^{-1}$  at the C/5 rate.

© 2007 Elsevier B.V. All rights reserved.

**Keywords:** Lead-acid battery; Specific energy; Graphite sheet; Polyaniline; Corrosion; Active-material shedding

### 1. Introduction

Lead-acid battery is one of the most successful electrochemical systems ever developed, and no other battery is yet able to compete with the lead-acid batteries on cost grounds, albeit batteries based on other chemistries are rapidly catching up [1]. In the past, although lead-acid battery designs have been optimized in several different ways, there are still certain new challenges faced by battery scientists and technologists, as additional failure modes have become evident in various modes of use [2]. Significant research and development efforts are currently underway to enhance the specific energy [3–15], which currently remains restricted to only about  $30\text{--}35 \text{ Wh kg}^{-1}$  at the C/5 rate, which is primarily due to the high mass density of lead.

A number of conductive materials have been suggested as direct substitutes for the lead current-collector (grid), as fillers for plastic composite materials, and as protective films that would offer corrosion protection to current-collectors made of lead or other metals. These materials include carbon, conductive ceramics such as Magnelli phases

of titanium oxide, transition oxides and barium metaplumbate, and glass fibres coated with conductive tin oxide [16].

Carbon is inert in sulfuric acid and hence could be used as a grid material for lead-acid batteries. Studies reported in the literature have demonstrated the suitability of graphite as a grid material [17–22]. Das and Mondal [19,20] have used lead and lead oxide coated graphite rods as electrodes in lead-acid cells, but the cells showed high self-discharge rates and limited cycles. Gyenge et al. [21] have employed electroplated vitreous carbon as a grid material for lead-acid cells with good cycle-life, wherein the lead coating was thicker (about  $200\text{--}400 \mu\text{m}$ ) to account for corrosion. Recently, the electrochemical stability of graphite foams as current-collectors for lead-acid batteries has been evaluated by Jang et al. [22]. This is an attractive proposition but further improvements are imperative for their commercial exploitation. As a part of an ongoing programme for enhancing the specific energy of lead-acid batteries [23–26], we report a basic study on lead-acid cells with flexible graphite grids that have been corrosion protected by coating polyaniline (PANI) electrochemically. The cells have a specific energy value of *ca.*  $40 \text{ Wh kg}^{-1}$  at the C/5 rate. In the literature [27–30], polyaniline has been used as a conductive polymer additive in positive plates of lead-acid cells. Recently, polyaniline has also been added to the negative plates [31].

\* Corresponding author. Tel.: +91 80 22933304; fax: +91 80 23601310.  
E-mail address: [pahari@sscu.iisc.ernet.in](mailto:pahari@sscu.iisc.ernet.in) (B. Hariprakash).

## 2. Experimental

Lead-acid battery grids of dimensions 40 mm × 60 mm × 2 mm were made from flexible graphite sheets obtained from M/s. Graphite India Ltd., Bangalore, India. The grids were then coated with a lead layer followed by a polyaniline (PANI) layer, as described elsewhere [25,26]. Powder X-ray diffraction (XRD) patterns for the graphite sheet and PANI layer were recorded on a Siemens D-5005 X-ray diffractometer using  $\text{CuK}\alpha$  radiation. The deposition of PANI was characterized by infrared spectroscopy on a Perkin-Elmer IR spectrometer. The surface morphologies of the graphite sheets and PANI layer were examined by means of JEOL JSM 840A scanning electron microscope. The electrochemical characteristics of the graphite sheet, lead layer and PANI were studied by cyclic voltammetry using  $\text{Pb/PbSO}_4$ ,  $\text{SO}_4^{2-}$  reference electrode (against which all potentials are reported) and an AUTOLAB PGSTAT 30 (Eco Chemie BV, Utrecht, The Netherlands) equipment with a BSTR10A current booster module.

Both the positive and negative plates of the lead-acid cell were prepared using graphite/Pb/PANI grids to construct several 2 V/1 Ah cells in a Plexiglas container filled with 1.25 rel. dens.  $\text{H}_2\text{SO}_4$  electrolyte following an established industrial protocol [24]. The cells were formed by galvanostatic charging and discharging with a Keithley 228A voltage/current source. Impedance measurements were performed on the cells in the frequency range between 10 kHz and 5 mHz by employing an AUTOLAB PGSTAT 30 instrument. The cells were subjected to charge–discharge studies at varying rates at 25 °C. The cells were also subjected to life-cycle tests at the C/3 rate at 25 °C.

Commercial grade 2 V/24 Ah lead-acid cells, with the corrosion-protected lightweight graphite grids of dimensions 152 mm × 118 mm × 2 mm both for positive and negative plates, were also assembled and tested. The graphite sheets were initially machined to a preferred grid structure (Fig. 1) by

means of a CNC Vertical Machining Center (BMV 45 TC20 with FANUC-0i MB, Bharat Fritz Werner Limited, Bangalore, India). The machined graphite grids were electroplated with lead (50  $\mu\text{m}$ ) followed by a corrosion-resistant PANI coating (5  $\mu\text{m}$ ). The corrosion-protected grids were then pasted with active materials and necessary conditions were maintained during curing and formation to alleviate premature capacity loss in the commercial-grade cells [32].

## 3. Results and discussion

The grids used in the present study were obtained by punching flexible graphite sheets that were manufactured from high-quality natural graphite flakes without any binder material. The graphite sheets have very good electrical and thermal conductivity and are resistant to electrochemical corrosion [33]. The mass density of such sheets ranges between 0.7 and 1.2  $\text{g cm}^{-3}$ . Those used in the present study have a mass density of about 1.1  $\text{g cm}^{-3}$  and the grids can be punched easily into different sizes and shapes. The grid structure used for the present study is shown schematically in Fig. 1.

Cyclic voltammograms (CVs) of a graphite sheet of dimensions 30 mm × 20 mm × 2 mm conducted over the operating voltage range of a lead-acid cell and at a sweep rate of 5  $\text{mV s}^{-1}$  are given in Fig. 2. Fig. 2(a) shows the CV of the graphite sheet between 1 and 2.7 V. The data suggest that the material could be used as a positive grid in lead-acid cells as oxygen gas evolution starts only at about 2.4 V, as is observed with conventional lead grids. Fig. 2(b) shows the CV of the grid in the potential regime between –0.5 and 0.5 V. It is seen that the negative active-material can be charged well within the hydrogen gas evolution region. This confirms the viability of the graphite grids for negative plates in lead-acid cells.

The cycle-life of the cells with bare graphite grids is rather limited because the electrolyte creeps inside the graphite layers and degrades the mechanical integrity of the grids. To mitigate this electrolyte creepage, the grids were electroplated with

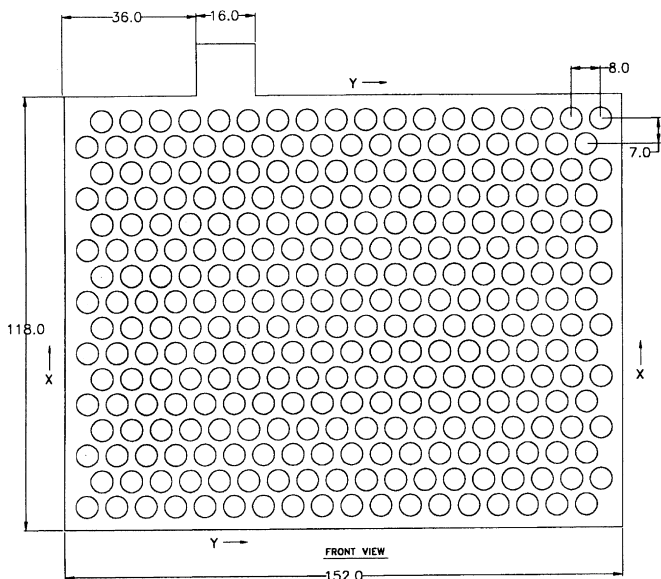


Fig. 1. Schematic representation of grid structure.

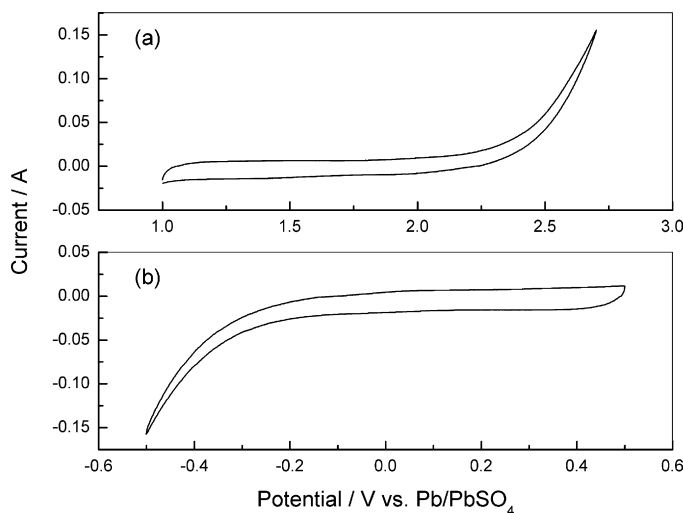


Fig. 2. Cyclic voltammograms of graphite sheets for (a) positive and (b) negative electrode potential windows with reference to  $\text{Pb/PbSO}_4$ ,  $\text{SO}_4^{2-}$  electrode.

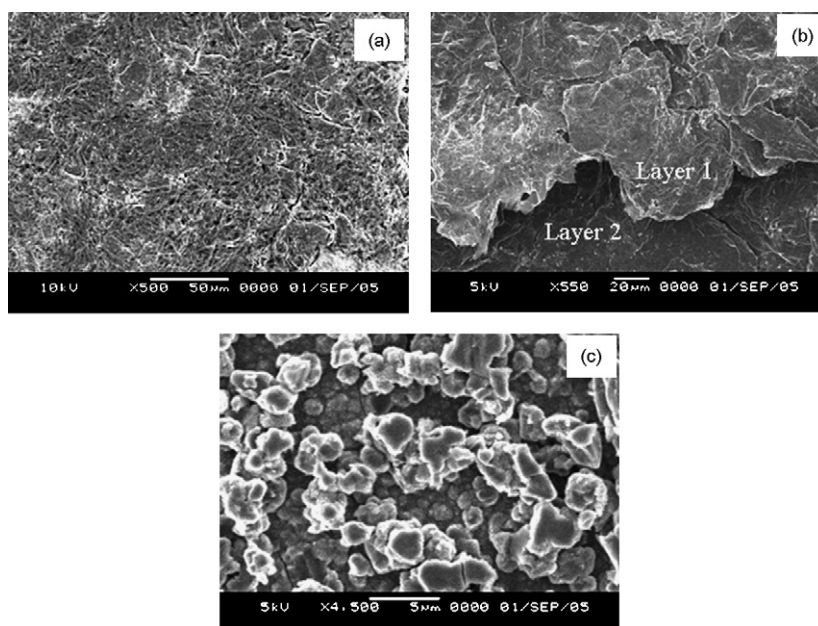


Fig. 3. Electron micrographs depicting surface morphologies of (a) outermost layer of graphite sheet, (b) inner layer of graphite sheet; (c) PANI film.

50  $\mu\text{m}$  of lead. The lead layer is subsequently coated electrochemically with a thin layer (5  $\mu\text{m}$ ) of polyaniline.

Electron micrographs of the graphite sheet and the PANI layer are given in Fig. 3. Fig. 3(a) shows the porous layer of graphite and Fig. 3(b) shows the inner graphite layers that facilitate electrolyte creepage and there by render the grids mechanically unstable. Fig. 3(c) shows the surface morphology of the porous PANI layer, which is composed of particles of size between 1 and 2  $\mu\text{m}$ .

The XRD patterns of highly ordered graphite and the porous PANI layer on the PANI coated graphite/lead grid substrate are presented in Fig. 4(a) and (b), respectively. The peaks present in Fig. 4(b) correspond to lead and thus indicate that the PANI layer is both amorphous and porous. In order to examine further the chemical nature of the PANI film, the IR spectrum

of the PANI film scrapped out from the grids was obtained, see Fig. 5. The spectrum shows: the following absorbance peaks: (a) at  $1592\text{ cm}^{-1}$ , corresponding to N=Q=N stretching; (b) at  $1511\text{ cm}^{-1}$ , corresponding to N–B–N stretching; (c) at  $1375\text{ cm}^{-1}$ , corresponding to C–N stretching in  $\text{QB}_t\text{Q}$ ; (d) at  $1250\text{ cm}^{-1}$ , corresponding to C–N stretching in  $\text{BBB}$ ; (e) at  $1128\text{ cm}^{-1}$ , corresponding to C–H in plane of bending 1,2,4-ring; (f) at  $950\text{ cm}^{-1}$ , corresponding to C–H out-of-plane bending with 1,2,4-ring; (g) at  $835\text{ cm}^{-1}$ , corresponding to C–H out-of-plane bending with 1,4 ring. In the aforesaid description, Q stands for the  $\text{C}_6\text{H}_4$ -ring in quinonoid form, B for the  $\text{C}_6\text{H}_4$  ring in benzenoid form, and  $\text{B}_t$  for *trans*-orientation of the  $\text{C}_6\text{H}_4$  ring in benzenoid form [34].

The CVs of graphite/Pb and graphite/lead/PANI grids of dimensions  $50\text{ mm} \times 30\text{ mm} \times 2\text{ mm}$  at a sweep rate of  $5\text{ mV s}^{-1}$

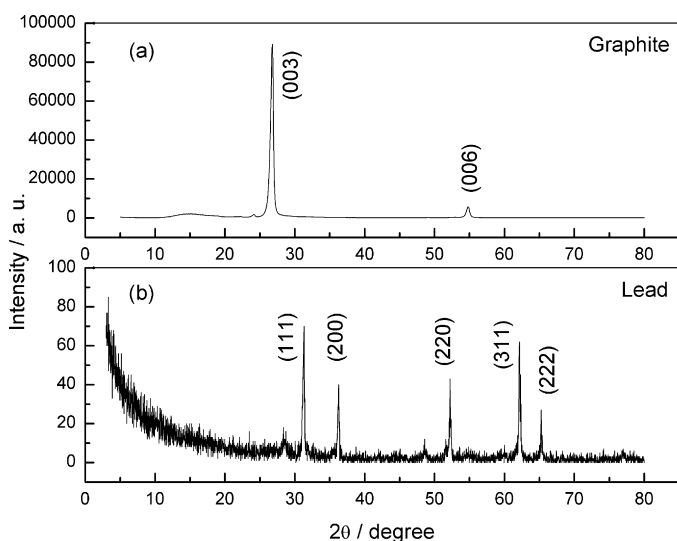


Fig. 4. Powder XRD patterns of (a) graphite sheet and (b) PANI film.

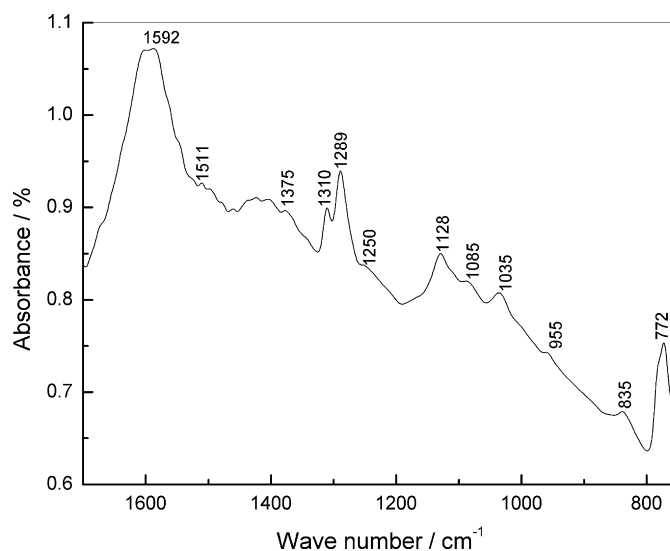


Fig. 5. Infrared spectrum of PANI film.

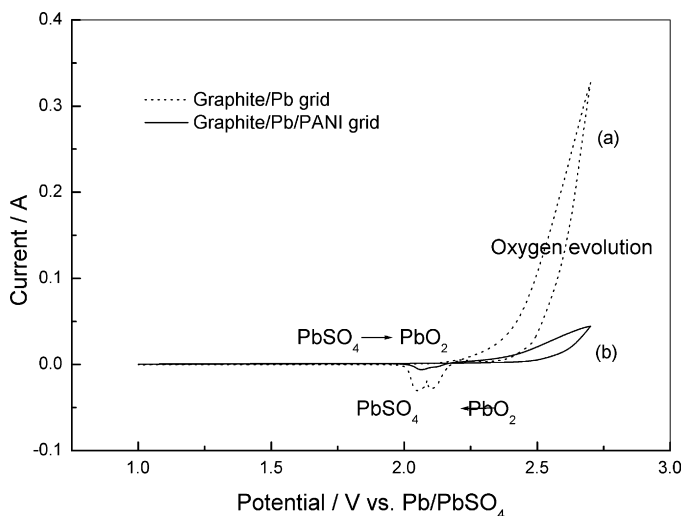


Fig. 6. Cyclic voltammograms of (a) graphite/Pb and (b) graphite/Pb/PANI grids.

are given in Fig. 6. The data clearly depict the oxidation of PbSO<sub>4</sub> to PbO<sub>2</sub> and the reduction of PbO<sub>2</sub> to PbSO<sub>4</sub>. It is noteworthy that the suppression of peak currents observed in graphite/Pb/PANI grids suggests a substantial reduction in lead corrosion. The CVs of graphite/Pb and graphite/Pb/PANI grids during the 1st and 20th cycles at a sweep rate of 5 mV s<sup>-1</sup> are shown in Fig. 7(a) and (b), respectively; a three-fold increment in the respective current value at 2.7 V for graphite/Pb grids in relation to graphite/Pb/PANI grids suggests that the latter are better suited for lead-acid battery grids in that they reduce grid-corrosion.

After confirming their suitability, the grids were pasted with positive and negative active-materials, followed by curing and drying. 2 V/1 Ah cells were assembled and the plates were soaked for about 2 h in aq. H<sub>2</sub>SO<sub>4</sub> prior to formation charging. During the first formation cycle, the cells were charged at the C/20 rate for 48 h followed by their discharge at C/10 rate. Subsequently, the cells were charged at the C/10 rate and discharged at

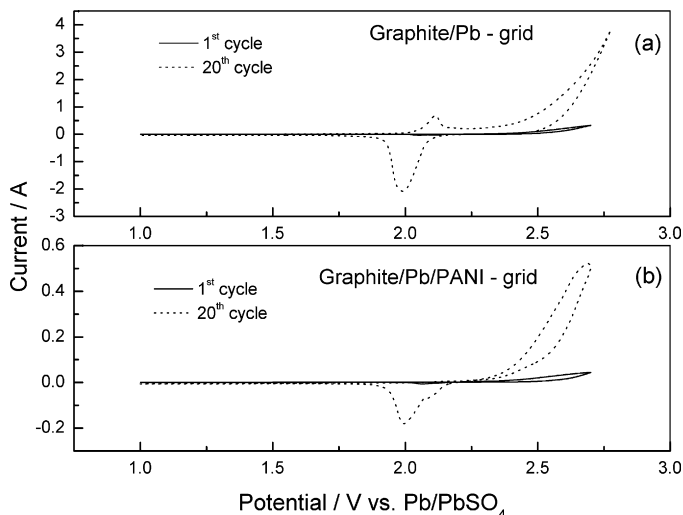


Fig. 7. Cyclic voltammograms of (a) graphite/Pb and (b) graphite/Pb/PANI grids at 1st and 20th cycles.

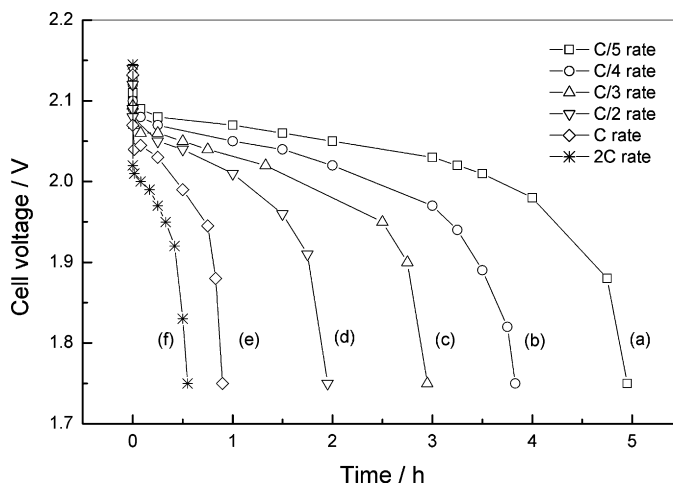


Fig. 8. Performance characteristics of 2 V/1 Ah lead-acid cell obtained at 25 °C at (a) C/5, (b) C/4, (c) C/3, (d) C/2, (e) C and (f) 2C rates.

the C/5 rate galvanostatically to complete the formation cycles. The cells are found to attain their maximum capacity within three cycles. The faradaic efficiency of the cells is about 80% at the C/5 rate at 25 °C, which is lower in relation to that of conventional cells. The performance characteristics of the cells at different rates between C/5 and 2C at 25 °C are shown in Fig. 8. The cells exhibit about 50% of the nominal capacity at the 2C rate as compared with their nominal capacity at the C/5 rate. The cells have a specific energy close to 40 Wh kg<sup>-1</sup> at the C/5 rate. The initial voltage drop observed during discharge suggests that the cells have a high internal resistance. Typical impedance data for the cells, subsequent to their formation, at various states-of-charge (SoCs) are presented in Fig. 9. The impedance parameters of the cells are evaluated from the experimental impedance spectrum employing the equivalent-circuit, non-linear least-square fitting procedure proposed by Boukamp [35]. The charge-transfer resistance of cells at SoCs of 1, 0.75, 0.5, 0.25 and 0 is 0.682, 0.564, 0.504, 0.699 and 0.931 Ω, respec-

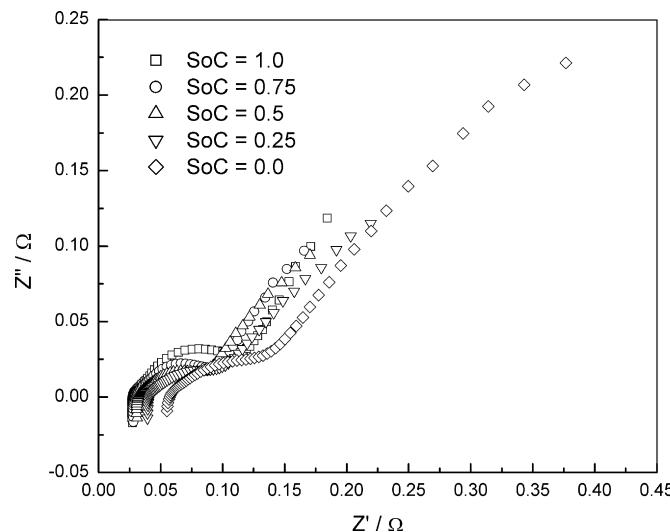


Fig. 9. Impedance data for 2 V/1 Ah lead-acid cell at various SoCs at 25 °C.



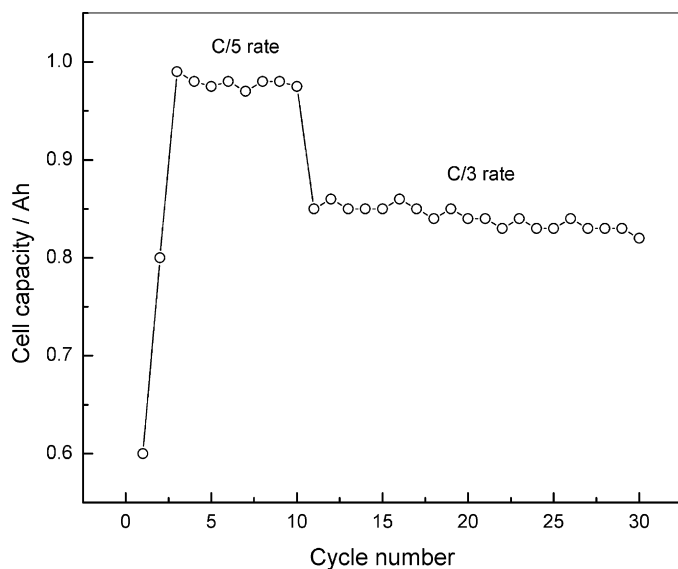


Fig. 10. Cycle-life data for 2 V/1 Ah lead-acid cell at 25 °C.

tively. The corresponding ohmic resistance is 0.027, 0.028, 0.031, 0.041 and 0.060  $\Omega$ , respectively. The data clearly suggest that the impedance values associated with the cells are comparatively higher than those of conventional cells. The cells were cycled at the C/3 rate for about 30 cycles and the data are shown in Fig. 10. The cell capacity decreases rapidly beyond 30 cycles due to active material shedding. The self-discharge rate of the cells is higher than that of conventional lead-acid cells at room temperature.

Active material shedding from both the positive and negative plates was found when the cells were cut open after 50 cycles to analyze the failure mechanism. Specifically, the active material pellets are loosely bound to the current-collector surface and this is responsible for the poor faradaic efficiency during the cycling. Exfoliation of the lead layer is also observed during cycling of the commercial-grade cells and is responsible for the capacity decay with cycling. This is due to the poor adhesion of the electroplated lead on the graphite sheet, probably because the graphite grids employed in the present study have smooth and shiny surfaces. Accordingly, it is necessary to improve the bonding strength of lead to the graphite.

#### 4. Conclusions

It has been possible to realize lead-acid cells with specific energy values close to 40 Wh kg<sup>-1</sup> with PANI coated graphite grids at the C/5 rate. Performance characteristics of the cells assembled from these grids are similar to those of conventional lead-acid cells. The present study suggests that lead-electroplated flexible graphite sheets may prove suitable as grid substrates for lead-acid batteries. Nevertheless, improvements in paste adhesion are imperative for commercial exploitation of such grids in lead-acid cells.

#### Acknowledgements

The authors are grateful to A. K. Shukla of the Solid State and Structural Chemistry Unit (SSCU), Indian Institute of Science (IISc), Bangalore, India, and to N. Gautam of NED Energy Ltd., Hyderabad, India for their support and encouragement. Thanks are also due to S.K. Martha, SSCU, IISc, Bangalore, India for undertaking the IR studies.

#### References

- [1] R.M. Dell, D.A.J. Rand, Understanding Batteries, Royal Society of Chemistry, Cambridge, UK, 2002.
- [2] D.A.J. Rand, P.T. Moseley, J. Garche, C.D. Parker, Valve-Regulated Lead-Acid Batteries, Elsevier, New York, 2004.
- [3] M.L. Soria, J. Fulla, F. Saez, F. Trinidad, J. Power Sources 78 (1999) 220.
- [4] R.H. Hammar, D.J. Harvey, US Patent 4,221,854 (1980).
- [5] N. Pinsky, S.A. Alkaitis, US Patent 4,713,306 (1987).
- [6] J.J. Rowlette, US Patent 5,643,696 (1997).
- [7] K. Tsuchida, H. Imai, US Patent 6,232,017 (2001).
- [8] J.B. Timmons, R. Bhardwaj, J.A. Orsino, US Patent 6,316,148 (2001).
- [9] I. Kurisawa, M. Shiomi, S. Ohsumi, M. Iwata, M. Tsubota, J. Power Sources 95 (2001) 125.
- [10] J.B. Timmons, J.A. Orsino, R. Bhardwaj, US Patent 6,447,954 (2002).
- [11] R.C. Bhardwaj, J. Than, J. Power Sources 91 (2000) 51.
- [12] G. Barkleit, A. Grahl, M. Maccangi, M. Olper, P. Scharf, R. Wagner, H. Warlimont, J. Power Sources 78 (1999) 73.
- [13] P.T. Moseley, R.D. Prengaman, J. Power Sources 107 (2002) 240.
- [14] J. Wang, H.K. Liu, S.X. Dou, S. Zhong, Y. Zhu, C. Fu, J. Power Sources 113 (2003) 241.
- [15] D.R. Battlebury, J. Power Sources 80 (1999) 7.
- [16] K.R. Bullock, J. Power Sources 51 (1994) 1, and references therein.
- [17] A. Czerwinski, M. Zelazowska, J. Electroanal. Chem. 410 (1996) 55.
- [18] A. Czerwinski, M. Zelazowska, J. Power Sources 64 (1997) 29.
- [19] K. Das, A. Mondal, J. Power Sources 55 (1995) 251.
- [20] K. Das, A. Mondal, J. Power Sources 89 (2000) 112.
- [21] E. Gyenge, J. Jung, B. Mahato, J. Power Sources 113 (2003) 388.
- [22] Y. Jang, N.J. Dudney, T.N. Tiegs, J.W. Klett, J. Power Sources 161 (2006) 1392.
- [23] S.A. Shivashankar, A.K. Shukla, A.U. Mane, B. Hariprakash, S.A. Gaffoor, US Patent 0151982 A1 (2004).
- [24] B. Hariprakash, A.U. Mane, S.K. Martha, S.A. Gaffoor, S.A. Shivashankar, A.K. Shukla, Electrochem. Solid-State Lett. 7 (2004) A66.
- [25] S.K. Martha, B. Hariprakash, S.A. Gaffoor, D.C. Trivedi, A.K. Shukla, Electrochem. Solid-State Lett. 8 (2005) A353.
- [26] A.K. Shukla, S.K. Martha, B. Hariprakash, S.A. Gaffoor, D.C. Trivedi, US Patent Application (2004).
- [27] P. Mirebeau, G. Chedeville, E. Genies, French Patent 2,553,581 (1985).
- [28] P. Mirebeau, French Patent 2,519,191 (1983).
- [29] M. Matsumoto, S. Ito, Jpn. Kokai Tokkyo Koho JP 61/455565A2 [86/45565] (1986).
- [30] K.R. Bullock, T.C. Dayton, in: D.A.J. Rand, P.T. Moseley, J. Garche, C.D. Parker (Eds.), Valve-Regulated Lead-Acid Batteries, Elsevier, New York, 2004, Chapter 4, pp. 119–120.
- [31] T. Funato, K. Takahashi, US Patent 5,547,783 (1996).
- [32] D. Pavlov, in: B. Hariprakash, T. Prem Kumar, A.K. Shukla (Eds.), Essentials of Lead-Acid Batteries, SAEST, Karaikudi, India, 2006, Chapter 3, pp. 33–61.
- [33] <http://www.graphiteindia.com/flexible.htm>.
- [34] S.K. Martha, B. Hariprakash, S.A. Gaffoor, A.K. Shukla, J. Appl. Electrochem. 36 (2006) 711.
- [35] B.A. Boukamp, Equivalent Circuit User Manual, University of Twente, The Netherlands, 1988/89.